

Approximate dispersion relations for qP – qSV -waves in transversely isotropic media

Michael A. Schoenberg* and Maarten V. de Hoop†

ABSTRACT

To decouple qP and qSV sheets of the slowness surface of a transversely isotropic (TI) medium, a sequence of rational approximations to the solution of the dispersion relation of a TI medium is introduced. Originally conceived to allow isotropic P -wave processing schemes to be generalized to encompass the case of qP -waves in transverse isotropy, the sequence of approximations was found to be applicable to qSV -wave processing as well, although a higher order of approximation is necessary for qSV -waves than for qP -waves to yield the same accuracy. The zeroth-order approximation, about which all other approximations are taken, is that of elliptical TI, which contains the correct values of slowness and its derivative along and perpendicular to the medium's axis of symmetry. Successive orders of approximation yield the correct values of successive orders of derivatives in these directions, thereby forcing the approximation into increasingly better fit at the intervening oblique angles. Practically, the first-order approximation for qP -wave propagation and the second-order approximation for qSV -wave propagation yield sufficiently accurate results for the typical transverse isotropy found in geological settings. After only slight modification to existing programs, the rational approximation allows for ray tracing, (f - k) domain migration, and split-step Fourier migration in TI media—with little more difficulty than that encountered presently with such algorithms in isotropic media.

INTRODUCTION

For velocity analysis and migration in transversely isotropic (TI) media, it is useful to have an algorithm that is simple (i.e., with the root structure of an isotropic medium) and accurate to calculate vertical slowness as a function of horizontal

slowness. In isotropic and vertical transversely isotropic (VTI) media, with no loss of generality, one can confine oneself to propagation in a single vertical plane. That plane is denoted here as the (x , z)-plane, with the z -direction taken as vertical. For an isotropic medium, the dispersion or slowness relation is of the form

$$s_z^2 = \frac{1}{\alpha^2} - s_x^2,$$

a straight line in the (s_x^2 , s_z^2) plane, where s_x is the horizontal slowness, s_z is the vertical slowness, and α is the medium's wave speed. For elliptical TI (a very special case), the slowness relation is also such a straight line, albeit with $\alpha = \alpha_V$ and with a different slope because of the difference between horizontal (H) and vertical (V) medium wave speeds.

In a general TI medium, each slowness curve in the (s_x^2 , s_z^2) plane is part of a conic section. For most rocks, the conic section is a hyperbola: one branch for the quasi- P (qP) dispersion relation and the other for the quasi- SV (qSV), the shear wave with polarization in the vertical plane. Although closed-form expressions for this hyperbola are known, they are not easy to work with because they involve a square root. So we are interested in understanding rational approximations of slowness surfaces in anisotropic media—in particular, for shear waves that exhibit singularities. In this paper, a sequence of expressions is derived, giving an approximate relation for s_z^2 as a sum of rational functions of s_x^2 and a dimensionless anellipticity parameter ϵ_A . The n th-order approximation has the form

$$s_z^2 = \frac{1}{\alpha_V^2} \left[1 - \alpha_H^2 s_x^2 + b_1 \frac{N(s_x^2) \epsilon_A}{D(s_x^2; \epsilon_A)} + b_2 \frac{N^2(s_x^2) \epsilon_A^2}{D^3(s_x^2; \epsilon_A)} + \dots + b_n \frac{N^n(s_x^2) \epsilon_A^n}{D^{2n-1}(s_x^2; \epsilon_A)} \right],$$

where the b_j are constants, $N = \alpha_H^2 s_x^2 (1 - \alpha_H^2 s_x^2)$, and D is a linear function of s_x^2 and ϵ_A . For weak anisotropy, by definition, only a single rational term is needed. For usual shales, which

Manuscript received by the Editor May 26, 1998; revised manuscript received September 21, 1999.

*Formerly Schlumberger-Doll Research, Old Quarry Road, Ridgefield, Connecticut 06877-4108; currently retired, 5 Mountain Rd., W. Redding, Connecticut 06896. E-mail: mike@PO-Box_307.ridgefield.sdr.slb.com.

†Colorado School of Mines, Center for Wave Phenomena, Golden, Colorado 80401-1887. E-mail: mdehoop@dix.mines.edu.

© 2000 Society of Exploration Geophysicists. All rights reserved.

often have significant positive anellipticity, one or at most two rational terms should be sufficient for the qP slowness relation, while two or at most three terms should be sufficient for the qSV slowness relation.

The approximations are based on the Taylor series expansion of $1 - \sqrt{1 - \zeta}$ in the small quantity ζ . The derivation of the approximations and their properties in the complex plane follow a discussion of mild anisotropy and the introduction of a set of dimensionless anisotropy parameters suitable to describing the anisotropic behavior at grazing and vertical incidence as well as at all angles in between.

The rational approximations are then compared with the slowness curve from Dellinger, Muir, and Karrenbach's elegant and quite accurate implicit bielliptic approximation (Dellinger et al., 1993) after a short discussion of its properties. Applications to f - k migration are then discussed. Approximate dispersion curves are shown for Greenhorn shale and for media which are perturbations to it.

EXACT DISPERSION RELATIONS

For a TI medium, the stress-strain relation in condensed notation is (Helbig and Schoenberg, 1986)

$$\begin{bmatrix} \sigma_{xx} \\ \sigma_{yy} \\ \sigma_{zz} \\ \sigma_{yz} \\ \sigma_{zx} \\ \sigma_{xy} \end{bmatrix} = \begin{bmatrix} \sigma_1 \\ \sigma_2 \\ \sigma_3 \\ \sigma_4 \\ \sigma_5 \\ \sigma_6 \end{bmatrix},$$

$$= \rho \begin{bmatrix} c_{11} & c_{11} - 2c_{66} & c_{13} & 0 & 0 & 0 \\ c_{11} - 2c_{66} & c_{11} & c_{13} & 0 & 0 & 0 \\ c_{13} & c_{13} & c_{33} & 0 & 0 & 0 \\ 0 & 0 & 0 & c_{55} & 0 & 0 \\ 0 & 0 & 0 & 0 & c_{55} & 0 \\ 0 & 0 & 0 & 0 & 0 & c_{66} \end{bmatrix} \begin{bmatrix} \epsilon_1 \\ \epsilon_2 \\ \epsilon_3 \\ \epsilon_4 \\ \epsilon_5 \\ \epsilon_6 \end{bmatrix}, \quad (1)$$

where, according to convention for condensed notation,

$$\begin{bmatrix} \epsilon_1 & \epsilon_2 & \epsilon_3 & \epsilon_4 & \epsilon_5 & \epsilon_6 \end{bmatrix} \equiv \begin{bmatrix} \epsilon_{xx} & \epsilon_{yy} & \epsilon_{zz} & 2\epsilon_{yz} & 2\epsilon_{zx} & 2\epsilon_{xy} \end{bmatrix}.$$

The c_{ij} are the stiffness moduli divided by density ρ , so they have dimension velocity²; hence, they are called the squared velocity moduli. For positive strain energy to be guaranteed, i.e., for the medium to be stable, the 6×6 elastic squared velocity matrix must be positive definite.

The Christoffel equations for plane waves with their polarization in the plane of propagation is (Helbig and Schoenberg, 1986)

$$\begin{bmatrix} c_{11}s_x^2 + c_{55}s_z^2 - 1 & (c_{55} + c_{13})s_x s_z \\ (c_{55} + c_{13})s_x s_z & c_{55}s_x^2 + c_{33}s_z^2 - 1 \end{bmatrix} \begin{bmatrix} u_x \\ u_z \end{bmatrix} = \begin{bmatrix} 0 \\ 0 \end{bmatrix}. \quad (2)$$

These equations completely describe qP - and qSV -wave propagation in the (x, z) plane, which depends only on the four squared velocity moduli: c_{11} , c_{33} , c_{55} , and c_{13} . The slowness curve for these waves is the solution of the dispersion relation, which expresses the vanishing of the determinant of the 2×2 matrix of coefficients acting on the polarization vector $[u_x, u_z]^T$ in equation (2). This dispersion relation is

$$c_{11}c_{55}(s_x^2)^2 + [(c_{11} + c_{33})c_{55} + E^2]s_x^2s_z^2 + c_{33}c_{55}(s_z^2)^2 - (c_{11} + c_{55})s_x^2 - (c_{33} + c_{55})s_z^2 + 1 = 0, \quad (3)$$

where

$$E^2 \equiv (c_{11} - c_{55})(c_{33} - c_{55}) - (c_{13} + c_{55})^2.$$

Note that E^2 , already introduced by Gassmann (1964), can be positive, negative, or zero but has the dimension of the square of squared velocity moduli and hence this notation. Also note that $c_{11} = c_{33}$ and $E^2 = 0$ are the necessary and sufficient conditions for P - SV -wave isotropy.

It is important to emphasize at this stage the physical interpretation of E^2 . First, the intersections of the slowness curves with the coordinate axes are fixed by the values of c_{11} , c_{33} , and c_{55} . These intersections with the coordinate axes may be called the anchor points. For the qP slowness curve, the anchor points are $[s_x, s_z] = [1/\sqrt{c_{11}}, 0]$ and $[0, 1/\sqrt{c_{33}}]$. For the qSV slowness curve, they are $[1/\sqrt{c_{55}}, 0]$ and $[0, 1/\sqrt{c_{55}}]$. The value of E^2 , which depends on the somewhat enigmatic modulus c_{13} , determines the shape of the slowness curves between the anchor points. The value E^2 increases as c_{13} decreases until $c_{13} + c_{55} = 0$. The value of E^2 does not depend on the sign of $c_{13} + c_{55}$. For still more negative values of c_{13} , E^2 starts to decrease again. Thus, the slowness curves and wavefronts are independent of the sign of $c_{13} + c_{55}$, although the polarization is strongly affected; $c_{13} + c_{55} < 0$ is associated with anomalous polarization (see Helbig and Schoenberg, 1986).

The value of E^2 controls the bulging of the slowness curves and hence the possible triplication of the qSV wavefront. The special case $E^2 = 0$ is the case of elliptical anisotropy. Then the qP slowness curve is an ellipse connecting the qP anchor points, while the qSV slowness curve is a circle connecting the qSV anchor points. When $E^2 > 0$, the qP slowness curve bulges from the ellipse connecting the qP anchor points (the plane waves are slower) between the anchor points, while $E^2 < 0$ implies that this slowness curve is pulled in from the ellipse (the plane waves are faster) between the anchor points. On the other hand, for the qSV slowness curve when $E^2 > 0$, the qSV slowness curve is pulled in from the circle that connects the qSV anchor points. If E^2 is large enough, that qSV curve is pulled in enough to allow it to become concave in an angular region centered on a given oblique direction. This concavity, or change in the sign of the curvature, is manifest in the qSV wavefront by the presence of triplication centered about that oblique direction. TI shales often exhibit such concave regions of the qSV slowness curve.

TI rocks almost always have $E^2 > 0$ (see Thomsen, 1986). Several physical mechanisms cause positive E^2 . Using equivalent media theory, we can show that for any TI medium that is equivalent in the long-wavelength limit to a stationary finely layered medium comprised of isotropic layers, not necessarily alternating, E^2 must be positive (e.g., Schoenberg, 1994). In addition, we can show (Schoenberg and Sayers, 1995) that in the

same limit, an isotropic medium in which are embedded a set of parallel linear slip planes with an axisymmetric compliance matrix gives E^2 with the same sign as $Z_T - Z_N$, where Z_T is the tangential compliance and Z_N is the normal compliance of the slip interfaces per unit distance perpendicular to the interfaces. [Schoenberg and Sayers (1995) conjecture that $Z_T > Z_N$ is a common but not necessary feature.] Thus, $E^2 = 0$ when $Z_T = Z_N$, which implies the traction and displacement discontinuity across the slip interfaces are collinear.

The fit of any approximation to the exact solution will not depend on the actual magnitudes of the four relevant elastic moduli but on the shape of the solution for the slowness curves, which can depend on at most three parameters. To this end, consider the following notation.

First, let C denote the arithmetic mean of c_{11} and c_{33} , i.e.,

$$C \equiv \frac{1}{2}(c_{33} + c_{11}). \quad (4)$$

The only dimensional parameter, C , provides the scaling required but has no effect on the shape of the solution to the dispersion relation.

Second, let γ denote the common vertical and horizontal shear velocity squared, normalized by C , i.e.,

$$\gamma \equiv c_{55}/C. \quad (5)$$

The value γ [unrelated to Thomsen's (1986) parameter used for the ellipticity of SH -waves] is the ratio of the square of the shear speed along the coordinate axes to the mean of the square of the compressional speeds along the coordinate axes, analogous to $(v_S/v_P)^2$ for isotropic media. [The symbol γ is also used in the converted wave literature to denote $\sqrt{c_{33}/c_{55}}$ (Thomsen, 1999).]

Third, let ϵ_P denote the relative difference between c_{11} , the horizontal qP velocity squared, and c_{33} , the vertical qP velocity squared, i.e.,

$$\epsilon_P \equiv \frac{\frac{1}{2}(c_{11} - c_{33})}{C}. \quad (6)$$

Since $c_{11}, c_{33} > 0$, $|\epsilon_P| < 1$. Positive ϵ_P denotes the usual case when the medium's horizontal P -wave speed is greater than its vertical P -wave speed. The value ϵ_P is a renormalized version of Thomsen's (1986) parameter, denoted here as ϵ^T :

$$\epsilon^T = \frac{c_{11} - c_{33}}{2c_{33}} = \frac{\epsilon_P}{1 - \epsilon_P} \quad \text{and} \quad \epsilon_P = \frac{\epsilon^T}{1 + \epsilon^T}.$$

Since the rational approximations will be seen to be applicable over the entire range of direction, out to horizontal, the use of ϵ_P , which is normalized symmetrically with respect to horizontal and vertical compressional moduli, is preferable here. For weak anisotropy, $\epsilon_P \approx \epsilon^T \ll 1$.

Fourth, let ϵ_A denote a normalized version of E^2 , such that its maximum value over all values of c_{13} , holding c_{11} , c_{33} , and c_{55} constant, is unity (assuming c_{11} and c_{13} are both greater than or both less than c_{55}), i.e.,

$$\epsilon_A \equiv \frac{E^2}{E_{\max}^2} = \frac{(c_{11} - c_{55})(c_{33} - c_{55}) - (c_{13} + c_{55})^2}{(c_{11} - c_{55})(c_{33} - c_{55})} \leq 1. \quad (7)$$

The minimum value of E^2 and ϵ_A occurs when $c_{13} + c_{55}$ is as large as possible. Since stability requires $c_{13}^2 < (c_{11} - c_{66})c_{33}$, and

since it is allowable for $c_{66} \rightarrow 0$, the absolute minimum value of ϵ_A is

$$\begin{aligned} \epsilon_{A\min} &= \frac{(c_{11} - c_{55})(c_{33} - c_{55}) - (\sqrt{c_{11}c_{33}} + c_{55})^2}{(c_{11} - c_{55})(c_{33} - c_{55})} \\ &= -c_{55} \frac{c_{11} + c_{33} + 2\sqrt{c_{11}c_{33}}}{(c_{11} - c_{55})(c_{33} - c_{55})} = -2\gamma \frac{1 + \sqrt{1 - \epsilon_P^2}}{(1 - \gamma)^2 - \epsilon_P^2}. \end{aligned} \quad (8)$$

However, a reasonable assumption for sedimentary rocks is that $c_{66} > c_{55}$. Then, letting $c_{66} \downarrow c_{55}$ from above, stability would require that $c_{13}^2 < (c_{11} - c_{55})c_{33}$, and the minimum value of ϵ_A becomes

$$\begin{aligned} \epsilon_{A\min} &= \frac{(c_{11} - c_{55})(c_{33} - c_{55}) - (\sqrt{(c_{11} - c_{55})c_{33}} + c_{55})^2}{(c_{11} - c_{55})(c_{33} - c_{55})} \\ &= -c_{55} \frac{c_{11} + 2\sqrt{(c_{11} - c_{55})c_{33}}}{(c_{11} - c_{55})(c_{33} - c_{55})} \\ &= -\gamma \frac{1 + \epsilon_P + 2\sqrt{1 - \epsilon_P^2} - \gamma(1 - \epsilon_P)}{(1 - \gamma)^2 - \epsilon_P^2}. \end{aligned} \quad (9)$$

Anellipticity parameter ϵ_A may be written in terms of Thomsen's parameters,

$$\epsilon_A = \frac{2c_{33}}{c_{11} - c_{55}} (\epsilon^T - \delta^T).$$

The key dimensionless parameter for time processing of qP -waves in TI media has been found by Alkhalifah and Tsvankin (1995) to be $\eta \equiv (\epsilon^T - \delta^T)/(1 - 2\delta^T)$, which is equivalent to $\delta^T = (\epsilon^T - \eta)/(1 + 2\eta)$. Thus, anellipticity parameter ϵ_A is related to η by

$$\epsilon_A = \frac{2c_{11}}{c_{11} - c_{55}} \frac{\eta}{1 + 2\eta}.$$

Since stability implies $1 + 2\eta > 0$, we see that $\epsilon_A, \epsilon^T - \delta^T$, and η are of the same sign. Note that ϵ_A depends explicitly on shear-wave velocity through c_{55} , whereas in η the c_{55} dependence is implicit (inside δ^T).

The parameters ϵ_P and ϵ_A specify the qP - qSV -wave anisotropy; the vanishing of both [together with the vanishing of a third anisotropy parameter proportional to $c_{66} - c_{55}$, associated with the (elliptical) SH -wave] implies isotropy. Each of these parameters controls different aspects of the anisotropy, and the effects can be seen clearly by letting these parameters vary independently.

From equations (4)–(7), the squared velocity moduli normalized by C may be written in terms of the dimensionless parameters γ , ϵ_P , and ϵ_A as

$$\begin{aligned} \frac{c_{11}}{C} &= 1 + \epsilon_P, & \frac{c_{33}}{C} &= 1 - \epsilon_P, & \frac{c_{55}}{C} &= \gamma, \\ \frac{c_{13}}{C} &= \pm \sqrt{[(1 - \gamma)^2 - \epsilon_P^2](1 - \epsilon_A)} - \gamma. \end{aligned} \quad (10)$$

In the next section, we will constrain the value of c_{13} so that only the positive root is allowed.

MILD ANISOTROPY

It is useful to impose a set of conditions to restrict the range of TI media considered. The restrictive conditions are not of the form that certain parameters are small enough so that squares of the parameters can be neglected, i.e., they are not conditions of weak anisotropy. The conditions limit the range of allowable elastic behavior while including the commonly assumed properties of geological TI media. Media satisfying this set of conditions—which are concerned with (1) the ratio of shear to compressional velocities, (2) polarization (or a stronger condition on apparent Poisson's ratio), and (3) triplication—are called mildly anisotropic (see, for example, Carrion et al., 1992). There are three conditions.

First, the slowest compressional wave along any coordinate axis is faster than the fastest shear wave along any coordinate axis, which is equivalent to

$$\max[c_{55}, c_{66}] < \min[c_{11}, c_{33}].$$

In terms of the dimensionless parameters (ignoring the constraint on c_{66}),

$$\gamma < 1 - |\epsilon_P|. \quad (11)$$

Second, in any direction if a longitudinal wave and a transverse wave polarized in the vertical plane exist, the longitudinal wave is always faster than the transverse wave. This essentially states that anomalous polarization is not allowed, which is equivalent to

$$c_{13} + c_{55} > 0 \quad (12)$$

(Helbig and Schoenberg, 1986). This provides no condition on ϵ_A , since that parameter is a function of $(c_{13} + c_{55})^2$, but it requires the use of the positive square root in the fourth of equations (10). A useful and somewhat stronger condition one might choose to impose is that, for a rod of the TI medium with its axis parallel to the symmetry axis, the Poisson's ratio is positive, which is equivalent to positive c_{13} . In terms of the dimensionless parameters, this is equivalent to

$$\epsilon_A < 1 - \frac{\gamma^2}{(1 - \gamma)^2 - \epsilon_P^2}, \quad (13)$$

which then supersedes inequality (12).

The simplest, third, condition concerning triplication is that there is no triplication and hence no concavity of the qSV slowness curve. However, recent evidence shows that shales often violate the no triplication criterion according to measurements on various shales, both in the laboratory [for example, on Greenhorn shale (Jones and Wang, 1981)] and in various case studies with in-situ measurements [for example, Miller et al. (1993)]. All the evidence for the presence of a concave region of the qSV slowness curve in certain shales occurs for the case of positive anellipticity ϵ_A , implying that the triplicating region is centered about an oblique direction (near 45°) between the vertical axis of symmetry and the horizontal axis.

This is not too serious for the rational approximations we are proposing, since the horizontal and vertical components of the squared qSV slowness (and thus of the qSV slowness in each quadrant) still have a one-to-one relationship, as demonstrated by the squared slowness curve in Figure 1a. This one-to-one relationship of the qSV curve still exists for moderately negative anellipticity (Figure 1b). Triplication near the axes is manifest by a positive slope of the qSV squared slowness curve at either the horizontal or vertical axis. Figure 1c shows a case of strong negative anellipticity that triplicates about both the horizontal and vertical axes. Thus, the mild anisotropy condition concerning the absence of qSV triplication defined here is that there is no triplication centered on either the vertical or the horizontal axis. No triplication about the vertical z -axis is equivalent to $c_{13} + c_{55} < \sqrt{c_{11}(c_{33} - c_{55})}$ or, in terms of ϵ_A ,

$$\epsilon_A > -\frac{c_{55}}{c_{11} - c_{55}} = -\frac{\gamma}{1 + \epsilon_P - \gamma} \equiv \epsilon_{A_{z \text{ no trip}}}.$$

No triplication about the horizontal x -axis is equivalent to $c_{13} + c_{55} < \sqrt{c_{33}(c_{11} - c_{55})}$, or

$$\epsilon_A > -\frac{c_{55}}{c_{33} - c_{55}} = -\frac{\gamma}{1 - \epsilon_P - \gamma} \equiv \epsilon_{A_{x \text{ no trip}}}.$$

[See, for example, Payton (1983).] For our purpose, these inequalities can be combined to yield

$$\epsilon_A > -\frac{c_{55}}{\max[c_{11}, c_{33}] - c_{55}} = -\frac{\gamma}{1 + |\epsilon_P| - \gamma} \equiv \epsilon_{A_{\text{no trip}}}. \quad (14)$$

For mild anisotropy, with the strong condition that c_{13} be positive and with the weak condition that no triplication occur about either of the coordinate axes, from inequalities (13) and (14) the restriction on anellipticity ϵ_A becomes

$$-\frac{\gamma}{1 + |\epsilon_P| - \gamma} < \epsilon_A < 1 - \frac{\gamma^2}{(1 - \gamma)^2 - \epsilon_P^2}. \quad (15)$$

NORMALIZED DISPERSION RELATIONS

When $E^2 = 0$, the two roots of quadratic equation (3) are

$$\begin{aligned} qP: \quad s_{zqP_0}^2 &= \frac{1 - c_{11}s_x^2}{c_{33}}; \\ qSV: \quad s_{zqSV_0}^2 &= \frac{1}{c_{55}} - s_x^2. \end{aligned} \quad (16)$$

Since our rational approximation will be taken about the case of zero anellipticity, equation (3) will be nondimensionalized by stretching the squared slowness axes suitably, i.e., differently for the qP or qSV slowness curve. In both cases, the curve in the stretched squared slowness plane about which we are perturbing will be a straight line connecting points $[0, 1]$ and $[1, 0]$. To this end, we set

$$\begin{aligned} qP: \quad X &\equiv c_{11}s_x^2, & Z &\equiv c_{33}s_z^2; \\ qSV: \quad X &\equiv c_{55}s_x^2, & Z &\equiv c_{55}s_z^2; \end{aligned} \quad (17)$$

so that either case (16) for $E^2 = 0$ reads $Z = 1 - X$. For nonzero E^2 , the dispersion relations in equation (3) become

$$qP: \frac{c_{55}}{c_{11}}X^2 + \left[\left(\frac{c_{55}}{c_{11}} + \frac{c_{55}}{c_{33}} \right) + \frac{E^2}{c_{11}c_{33}} \right]XZ + \frac{c_{55}}{c_{33}}Z^2 - \left(1 + \frac{c_{55}}{c_{11}} \right)X - \left(1 + \frac{c_{55}}{c_{33}} \right)Z + 1 = 0; \quad (18)$$

$$qSV: \frac{c_{11}}{c_{55}}X^2 + \left[\frac{c_{11} + c_{33}}{c_{55}} + \frac{E^2}{c_{55}^2} \right]XZ + \frac{c_{33}}{c_{55}}Z^2 - \left(1 + \frac{c_{11}}{c_{55}} \right)X - \left(1 + \frac{c_{33}}{c_{55}} \right)Z + 1 = 0.$$

Now, let

$$Z = 1 - X + f(X; E^2). \quad (19)$$

With $f(X; 0) = 0$, note that for $E^2 = 0$ we indeed obtain the straightline solutions $Z = 1 - X$. Substituting equation (19) into equation (18) yields a quadratic equation in the perturbation f about the elliptically anisotropic case,

$$f^2 - B(X; \delta)f + \delta X(1 - X) = 0, \quad (20)$$

in which

$$qP: \delta \equiv \frac{E^2}{c_{11}c_{55}} = \frac{(1 - \gamma)^2 - \epsilon_p^2}{\gamma(1 + \epsilon_p)}\epsilon_A,$$

$$B(X; \delta) \equiv \frac{c_{33}}{c_{55}} - 1 + \left(1 - \frac{c_{33}}{c_{11}} - \delta \right)X = \frac{1 - \gamma - \epsilon_p}{\gamma} + \left(\frac{2\epsilon_p}{1 + \epsilon_p} - \delta \right)X,$$

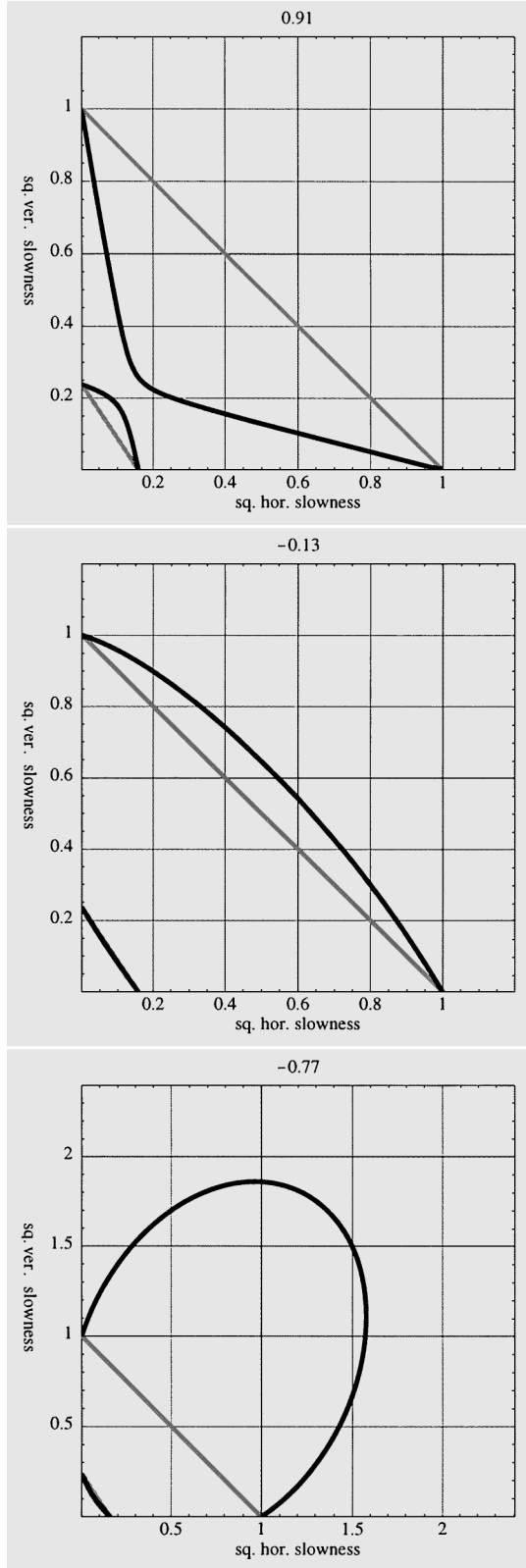
$$qSV: \delta \equiv \frac{E^2}{c_{33}c_{55}} = \frac{(1 - \gamma)^2 - \epsilon_p^2}{\gamma(1 - \epsilon_p)}\epsilon_A,$$

$$B(X; \delta) \equiv -\left(1 - \frac{c_{55}}{c_{33}} \right) + \left(1 - \frac{c_{11}}{c_{33}} - \delta \right)X = -\frac{1 - \gamma - \epsilon_p}{1 - \epsilon_p} - \left(\frac{2\epsilon_p}{1 - \epsilon_p} + \delta \right)X.$$

Regarding the expressions for B , first note that $B(0; \delta)$ is independent of δ and hence may be written as $B(0)$. In view of mild anisotropy condition (11), simple substitution shows that for qP , $B(0)$ is positive and $B(1; \delta)$ is positive for all δ .



FIG. 1. Squared slowness curves denoted by the solid black lines for three different TI media. All three media have $\gamma = 0.19$ and $\epsilon_p = 0.20$. For reference, the elliptical TI medium curves $\epsilon_A = 0$ (straight lines in the squared slowness domain) for the same γ and ϵ_p are the gray lines. (a) Positive anelasticity medium, with $c_{13} = 0.24$ equivalent to $\epsilon_A = 0.91$. (b) Moderate negative anelasticity medium, with $c_{13} = 3.39$ equivalent to $\epsilon_A = -0.13$. (c) Strong negative anelasticity medium, with $c_{13} = 4.50$ equivalent to $\epsilon_A = -0.77$, exhibits shear-wave triplication about both the vertical and horizontal axes. In this and all other figures, all slownesses are normalized by $\sqrt{c_{55}}$, so the anchor points of the qSV curves are always $[0, 1]$ and $[1, 0]$.



Similarly, for qSV , $B(0)$ is negative and $B(1; \delta)$ is negative for $\epsilon_A > \epsilon_{A_x \text{ no trip}}$, i.e., in the range of ϵ_A such that there is no triplication centered on the horizontal axis, this condition being subsumed in equation (14). Thus, subject to mild anisotropy,

$$B(X; \delta) \neq 0, \quad 0 \leq X \leq 1, \quad (21)$$

i.e., over the entire precritical range of X . For qP , B is positive over this range; for qSV , B is negative.

Of the two roots of quadratic equation (20), we want the one that vanishes when $\delta X(1 - X) = 0$ [then $f(X; 0) = 0$], i.e.,

$$f = \frac{1}{2}[B(X; \delta) - \chi(B(X; 0))\sqrt{B^2(X; \delta) - 4X(1 - X)\delta}], \quad (22)$$

where

$$\chi(\xi) \equiv \begin{cases} +1 & \text{if } \text{Re}\{\xi\} > 0, \\ -1 & \text{if } \text{Re}\{\xi\} < 0. \end{cases}$$

For the purpose of a Taylor expansion of the square root, we rewrite the root as follows:

$$f = \frac{B(X, \delta)}{2} \left[1 - \chi(B(X; 0))\chi(B(X; \delta)) \times \sqrt{1 - \frac{4X(1 - X)\delta}{B^2(X; \delta)}} \right]. \quad (23)$$

This expression shows more explicitly how branch cuts form.

Note that quadratic equations (18) for the qP - and qSV -waves can be written conveniently in terms of the appropriate δ and $B(X; \delta)$ by substituting $f \equiv X + Z - 1$ into equation (20). This substitution yields

$$F(X, Z; \delta) \equiv (X + Z - 1)^2 - B(X; \delta)(X + Z - 1) + \delta X(1 - X) = 0 \quad (24)$$

as the normalized form of the exact dispersion relation. This form is most suitable for expressing derivatives

$$\left. \frac{d^n Z}{dX^n} \right|_{X=0, Z=1} \quad \text{and} \quad \left. \frac{d^n X}{dZ^n} \right|_{X=1, Z=0}$$

in terms of δ and B , since $X + Z - 1$ vanishes both at $X = 0, Z = 1$ and at $X = 1, Z = 0$. In particular, from setting the total derivative of F with respect to X and with respect to Z to zero,

$$\left. \frac{dZ}{dX} \right|_{X=0, Z=1} = -1 + \frac{\delta}{B(0)}, \quad (25)$$

$$\left. \frac{dX}{dZ} \right|_{X=1, Z=0} = -1 + \frac{\delta}{B(1; 0)}.$$

Similarly, from differentiating F once again and setting the second-order total derivatives to zero, we find

$$\left. \frac{d^2 Z}{dX^2} \right|_{X=0, Z=1} = \frac{2\delta[\delta - B(0)B(1; \delta)]}{B^3(0)}, \quad (26)$$

$$\left. \frac{d^2 X}{dZ^2} \right|_{X=1, Z=0} = \frac{2\delta[\delta - B(0)B(1; \delta)]}{B^3(1; 0)}.$$

These expressions will be compared with analogous expressions based on the approximation to be developed below.

RATIONAL APPROXIMATIONS FOR SQUARED SLOWNESS CURVES

Expanding the square root in equation (23) in a Taylor series in $\delta X(1 - X)$ and limiting the number of terms yield a sequence of approximations that apply for small $X(1 - X)$ (i.e., simultaneously about near-vertical and near-critical horizontal slowness) and/or for small δ . If the series converges globally over the full real slowness surface, these approximations differ essentially from a parabolic approximation, as the appropriate conditions are satisfied at grazing incidence as well as at vertical incidence. If not, and the series diverges in some range between vertical and grazing incidence, the approximation would be similar to biparabolic about vertical and grazing incidence.

Now, Taylor expanding the square root expression of equation (23) yields, for f , the following series of rational functions of X :

$$f = \frac{B(X; \delta)}{2} \left[1 - \chi(B(X; \delta))\chi(B(X; 0)) \times \left(1 - \sum_{n=1}^{\infty} \frac{[2X(1 - X)\delta]^n}{n!B^{2n}(X; \delta)} \prod_{m=1}^n |2m - 3| \right) \right]$$

$$= \frac{B(X; \delta)}{2} \left[1 - \chi(B(X; \delta))\chi(B(X; 0)) \times \left(1 - \frac{2X(1 - X)\delta}{B^2(X; \delta)} - \frac{2[X(1 - X)\delta]^2}{B^4(X; \delta)} - \dots \right) \right] \quad (27)$$

and hence, from equations (19) and (17), the series for the squared vertical slownesses. This series converges globally only so long as

$$\left| \frac{4X(1 - X)\delta}{B^2(X; \delta)} \right| < 1. \quad (28)$$

The issue of convergence is relevant for precritical directions of propagation, i.e., on the interval $0 < X < 1$. Further, a pole in Z , and hence an algebraic branch point in s_z , is introduced by the approximation at $X = X_p$; X_p satisfies $B(X_p, \delta) = 0$. From equation (21) and the discussion preceding it, X_p cannot lie on the precritical interval between 0 and 1. The branch point will lie on the real axis (beyond the critical horizontal slowness) or on the imaginary axis in the complex horizontal slowness plane.

The branches of the elliptic, zeroth-order approximation (the straight lines in the squared slowness domain) cross at $X = X_x$ such that $B(X_x; 0) = 0$ for both qP and qSV . This crossing point is

$$s_x^2 = -\frac{c_{33} - c_{55}}{c_{55}(c_{11} - c_{33})}, \quad s_z^2 = -\frac{c_{11} - c_{55}}{c_{55}(c_{11} - c_{33})}. \quad (29)$$

At this point, the function $\chi(B(X; 0))$ in equation (23) changes sign and the rational approximation jumps from one branch or root to the other. For $c_{11} > c_{33}$, the jump occurs on the imaginary

horizontal slowness axis; for $c_{11} < c_{33}$, it occurs on the real horizontal slowness axis beyond critical qSV slowness. These jumps are necessary for the asymptotic behavior of the approximations at infinity in the complex horizontal slowness plane to be consistent with (although not exactly equal to) the asymptotic behavior of the exact solution. In particular, along the imaginary axis in the complex horizontal slowness plane, i.e., $X \rightarrow -\infty$, the vertical slowness $Z \rightarrow \infty$. This is of practical importance if these rational approximations are to be applied over a range of pre- and postcritical horizontal slowness. The right asymptotic behavior guarantees the convergence of the propagator in the space-time domain based on the spectral-domain approximation of, for example, de Hoop and de Hoop (1994).

As far as inequality (28) is concerned, there are two cases to consider: $\delta > 0$ (positive anellipticity) and $\delta < 0$ (negative anellipticity). Since the quadratic equation for f has two distinct real roots for all X , $0 < X < 1$, the expression in the square root of equation (23) is positive. Further, for $\delta > 0$, it has the form one minus the positive quantity in equation (28). Thus, that positive quantity must be less than unity. Hence, only the case $\delta < 0$ requires further analysis to find conditions for which equation (28) is satisfied; this analysis is carried out in Appendix A.

Now consider the precritical directions of propagation. The first-order approximation to either the qP or qSV slowness curve is returned by retaining just the first term in equation (27),

$$\begin{aligned} Z &= 1 - X + f = 1 - X + \frac{X(1 - X)\delta}{B(X; \delta)} \\ &= (1 - X) \frac{B(X; 0)}{B(X; \delta)} \equiv (1 - X)R_1(X), \end{aligned} \quad (30)$$

defining R_1 . The second-order approximation is returned by retaining the first two terms,

$$\begin{aligned} Z &= 1 - X + \frac{X(1 - X)\delta}{B(X; \delta)} + \frac{[X(1 - X)\delta]^2}{B^3(X; \delta)} \\ &= (1 - X) \frac{B(X; 0)B^2(X; \delta) + X^2(1 - X)\delta^2}{B^3(X; \delta)} \\ &\equiv (1 - X)R_2(X), \end{aligned} \quad (31)$$

defining R_2 . These expressions are the key results of this paper and the use of the definitions of X , B , and δ given by equations (17) and (20) converts them to equivalent expressions in terms of the elastic moduli. The n th-order approximation has the form $Z = (1 - X)R_n(X)$. Thus, the difference between isotropic processing and TI processing is that $R_n(X)$ must be included under the square root whenever one needs to find vertical slowness as a function of horizontal slowness.

The first-order expression satisfies the correct curvature at both normal and grazing incidence; the second-order expression additionally satisfies the correct third derivative of the slowness at normal and grazing incidence. Note that the curvatures of the slowness surface and the wavefront are reciprocal, while the curvature of the wavefront determines the short-spread moveout velocity; hence, matching the curvatures implies matching the zero-offset moveout velocities for both a horizontal and a vertical array of receivers. Higher order ap-

proximations satisfy higher order derivatives at normal and grazing incidence. The n th-order rational function $R_n(X)$ has $2n - 1$ degree polynomials in X for both numerator and denominator, with the denominator given by $B^{2n-1}(X; \delta)$.

It is important to point out that the approximation to a given order for the qSV curve is not as accurate as the one for the qP curve (because of the difference in maximum distance of the slowness curves to their ellipses). To achieve the same degree of accuracy for qSV , more terms must be taken into account. Each additional term matches the next higher derivative at $X = 0$, $Z = 1$, and $X = 1$, $Z = 0$. If, for example, one wished only to match the curvature (second derivative) of the slowness surface, one could add to the first-order rational approximation the second-order rational approximation term times a scaling factor chosen so that either (a) a given point between $X = 0$ and $X = 1$ is matched exactly or (b) a set of points between $X = 0$ and $X = 1$ is matched in an optimum way by a least-squares criterion. Thus, the third derivative at the endpoints will be slightly off in return for a much closer fit in the intermediate region between the axes. This is equivalent to an interpolation approach using a higher order correction term.

Other expansions

The square root in equation (23) can be expanded in several different ways. One could consider a power series in X , which would be fine near vertical; but such an expansion and others like it are not considered here because we are looking for approximations that are valid over the entire range $0 \leq X \leq 1$. A naive application of a power series in X never even gives $Z|_{X=1} = 0$.

Another possibility is to expand the series in equation (27) in a power series in δ , yielding

$$f = \frac{1 - X}{B(X; 0)}X\delta + \frac{1 - X}{B^3(X; 0)}[1 - X + B(X; 0)]X^2\delta^2 + \dots \quad (32)$$

Retaining only the first term yields

$$Z = (1 - X) \left[1 + \frac{X}{B(X; 0)}\delta \right],$$

which gives the exact value for $dZ/dX|_{X=0}$ but not for $dX/dZ|_{X=1}$. The power of the proposed rational approximation is that even a single term gives so much of the character of the exact slowness curve.

A simplification of the qP slowness relation

The qP slowness relation depends strongly on $c_{13} + 2c_{55}$ but only weakly on c_{13} or c_{55} individually. Hence, we are led to introduce the ratio

$$\lambda = \frac{c_{13}}{c_{13} + 2c_{55}}. \quad (33)$$

We express c_{13} and c_{55} in terms of the combination $a \equiv c_{13} + 2c_{55}$ and λ :

$$c_{55} = \frac{1}{2}(1 - \lambda)a, \quad c_{13} = \lambda a. \quad (34)$$

Then

$$E^2 = c_{11}c_{33} - \frac{1}{2}(1 - \lambda)a(c_{11} + c_{33}) - \lambda a^2. \quad (35)$$

In terms of λ and a , the dispersion relation (3) becomes

$$\begin{aligned} & [c_{11}s_x^2 + \frac{1}{2}(1-\lambda)as_z^2 - 1][\frac{1}{2}(1-\lambda)as_x^2 + c_{33}s_z^2 - 1] \\ & - [\frac{1}{2}(1+\lambda)a]^2 s_x^2 s_z^2 = 0. \end{aligned} \quad (36)$$

The qP slowness relation can be shown to be insensitive to variations in λ . The mild anisotropy conditions imply that $\lambda > -1$ and that $a > 0$. Also, mildly anisotropic media satisfy $c_{55} = \frac{1}{2}(1-\lambda)(c_{13} + 2c_{55}) < \min[c_{11}, c_{33}]$. If c_{55} and c_{66} are allowed to approach zero with a held equal to its original value, then $c_{13} > 0$ and $\lambda \uparrow 1$. In this acoustic limit, the exact dispersion relation for qP -waves simplifies [see equation (18)] to

$$\left[1 - \left(1 - \frac{a^2}{c_{11}c_{33}} \right) X \right] Z = 1 - X, \quad (37)$$

directly leading to a rational approximation. In terms of the parameters λ and a , our first-order rational approximation (30) becomes

$$\begin{aligned} Z &= (1 - X) \\ &\times \frac{1 - \frac{1}{2}(1-\lambda)\frac{a}{c_{33}} \left[1 - \left(1 - \frac{c_{33}}{c_{11}} \right) X \right]}{1 - \frac{1}{2}(1-\lambda)\frac{a}{c_{33}} + \left[(1-\lambda)\frac{a}{c_{33}} + \left(1 - \frac{\lambda a^2}{c_{11}c_{33}} \right) \right] X}, \end{aligned} \quad (38)$$

which in the limit $\lambda \uparrow 1$ reduces to the solution of the exact dispersion relation (37).

EXAMPLES

The approximations will be illustrated using the measured moduli of Greenhorn shale (Jones and Wang, 1981) as a starting model. The relevant squared velocity moduli in $(\text{km/s})^2$,

$$c_{11} = 14.47, \quad c_{33} = 9.57, \quad c_{55} = 2.28, \quad c_{13} = 4.51,$$

give dimensionless parameters

$$\gamma = 0.190, \quad \epsilon_P = 0.204, \quad \epsilon_A = 0.482.$$

Other examples considered have these same parameters except for anellipticity ϵ_A , which varies by changing the value of c_{13} . Thus, all examples have the same anchor points but different anellipticity. We compare the first- and second-order rational approximations with the exact slowness surfaces, with Dellinger et al.'s (1993) bielliptic approximation (derived in Appendix B), and with the elliptical TI medium. All examples conform to mild anisotropy.

Figure 2a shows the exact qP and qSV slowness curves, their first-order rational approximations, and their bielliptic approximations for Greenhorn shale. As a reference, for this figure and all the remaining figures, the associated elliptically anisotropic medium curves are shown in gray. Figure 2b shows, instead of the rational first-order approximation, the second-order approximation. This and subsequent figures are normalized so the qSV -curve traverses points $[0, 1]$ and $[1, 0]$, i.e., the curves are scaled by normalizing all moduli by c_{55} .

Next, we perturb the Greenhorn shale by increasing ϵ_A to the value 0.910 (by decreasing c_{13} to 0.547), Figure 3 shows the the same curves for this very anelliptic medium as were plotted in Figure 2. Figure 3a contains the first-order rational approximation, and Figure 3b contains the second-order approximation. In Figure 3c, approximation (37) is compared with the first-order rational approximation for qP -waves only. Finally, we perturb the Greenhorn shale by decreasing ϵ_A to the negative value -0.126 (by increasing c_{13} to 7.72). The slowness curves are shown in Figure 4.

For all three cases, the first-order rational approximation is very accurate for the qP curves while the second-order approximation is acceptable for the qSV curves, even for the very high anellipticity case shown in Figure 3. For all three cases, the first-order rational approximation is closer to the exact dispersion

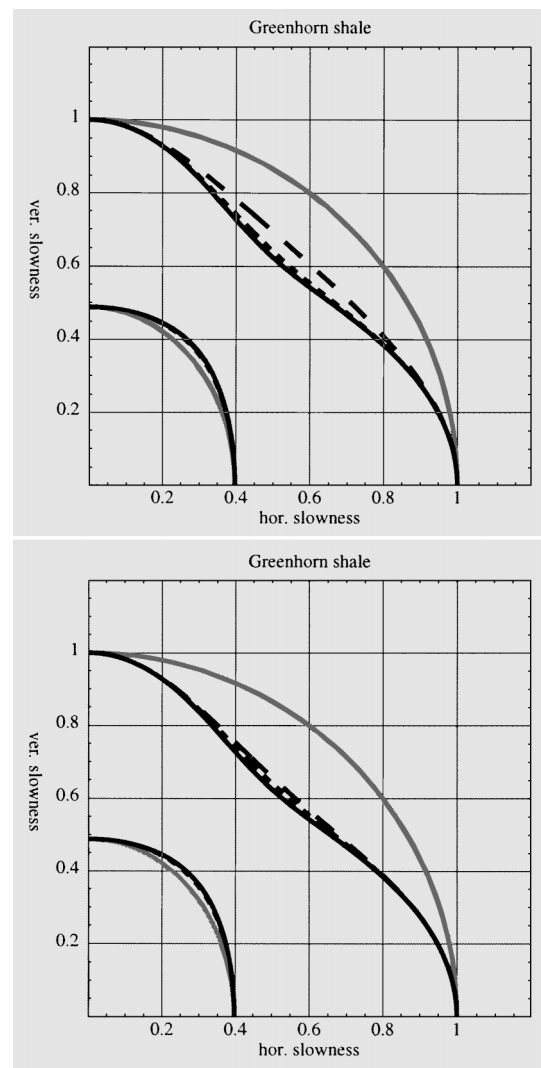


FIG. 2. Slowness curves for Greenhorn shale. The elastic moduli are normalized by c_{55} . The dimensionless parameters are $\gamma = 0.190$, $\epsilon_P = 0.204$, $\epsilon_A = 0.482$. The exact slowness curves are the black solid curves; the rational approximations are the long dashes; Muir's bielliptic approximations are the short dashes. For reference, the associated elliptical TI curves are shown in gray. (a) First-order rational approximation. (b) Second-order rational approximation.

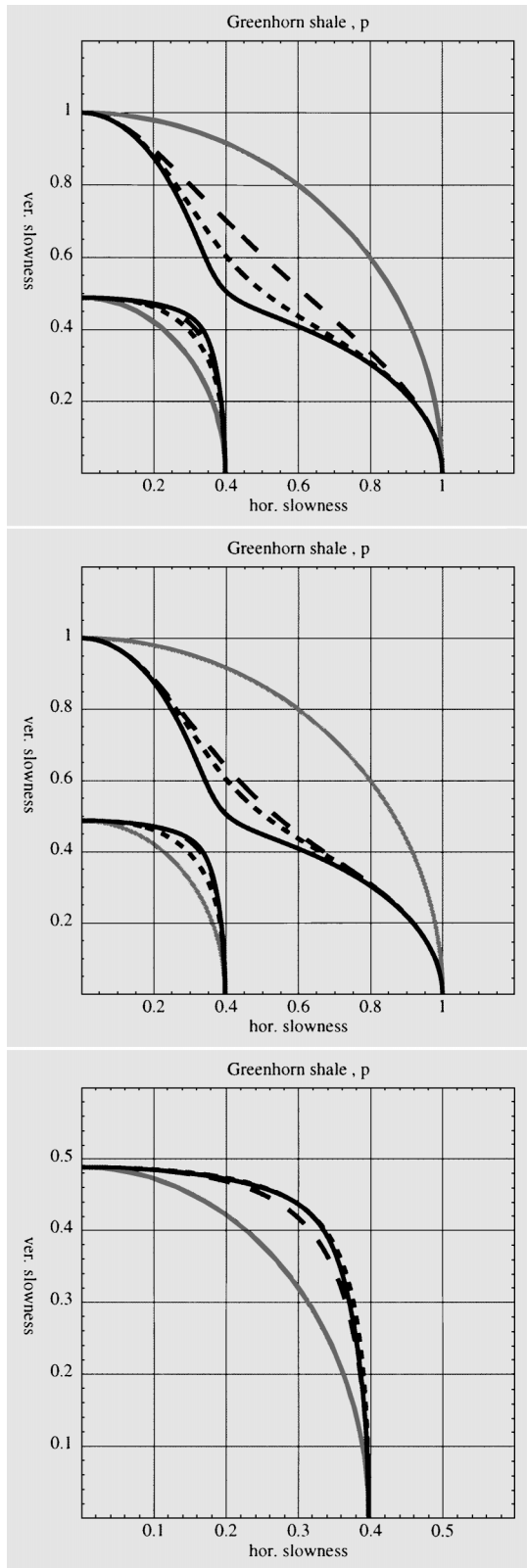


FIG. 3. Same as Figure 2 except the medium is a perturbed Greenhorn shale with anellipticity parameter ϵ_A increased to 0.910. (c) A comparison between the first-order rational approximation (long dashes) and the rational approximation (short dashes) based upon setting $\lambda = 0$ for qP -waves.

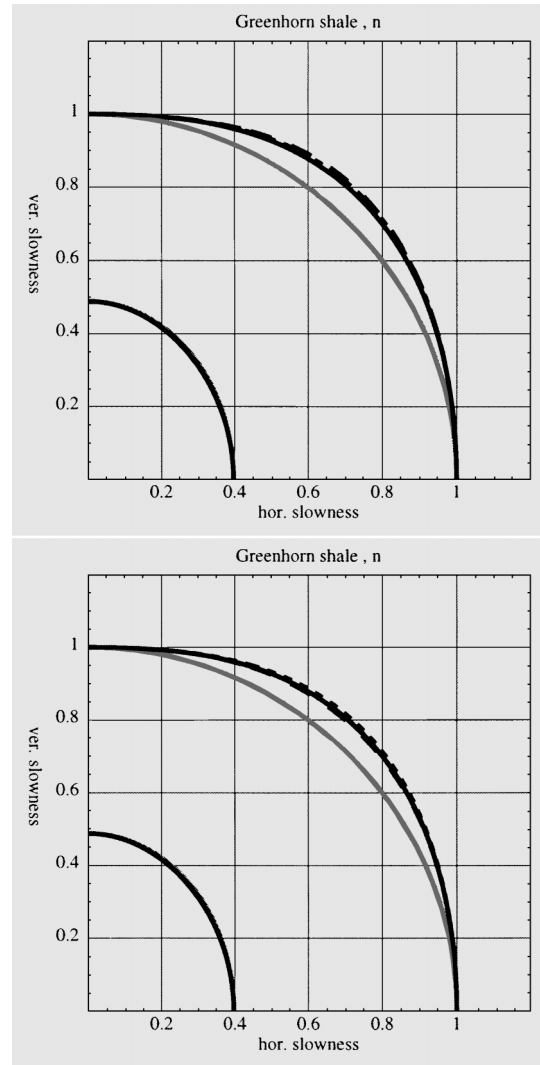


FIG. 4. Exactly as Figure 2 except the medium is a perturbed Greenhorn shale with negative anellipticity; ϵ_A is decreased to -0.126 .

relation than the bielliptic relation for qP but further for qSV . Even the second-order rational approximation only approaches (but not quite attains) the accuracy of the bielliptic approximation for qSV . The bielliptic approximation too can be generalized to satisfy higher order derivatives at the origin, although this is somewhat tedious. For positive anellipticity, the higher order rational approximations approach the exact curves monotonically from inside for qP and from outside for qSV . For negative anellipticity, if a given order approximation is inside the exact curve, the next order approximation will be outside, and vice versa. This is to be expected because the series expansion of equation (27) is an alternating series for $\delta < 0$. This can be seen in Figure 4 for the qSV curve.

Figure 5 shows slowness curves of a TI medium with large c_{55} (relative to c_{511} and c_{33}), specified by γ , and large negative anellipticity, specified by ϵ_A . The dimensionless parameters are

$$\gamma = 0.5, \quad \epsilon_P = 0.2, \quad \epsilon_A = -0.7143.$$

For the values of γ and ϵ_P , incipient triplication centered on the vertical occurs at just this value of ϵ_A , as can be seen by the zero curvature of the exact and approximate curves at the vertical axis. Divergence of series expansion (27) for the qSV surface for some X occurs for the less negative value of $\epsilon_A < -0.4545$. At this much greater negative value of ϵ_A , qSV divergence occurs for $0.338 < s_x < 0.902$. The figure shows the first-, fifth-, and ninth-order rational approximations. The qP curve converges everywhere, and even the first-order approximation is quite accurate. The approximate qSV curves in the divergence interval move away from the exact curve as the order increases.

In Figures 6 and 7 segments of the exact dispersion curve and the first-order rational approximation are shown which correspond to X lying out of the range $[0, 1]$. The behavior is illustrated for Greenhorn shale. In Figure 6, the vertical slowness is imaginary (corresponding to negative Z) along the real horizontal slowness axis beyond the critical angles (corresponding to $X > 1$). Note the singularity for the qP curve at $s_x = 0.725$, which is associated with $B_{qP}(X; \delta) = 0$. In Figure 7, the horizontal slowness is imaginary (corresponding to negative X). Note the singularity for the qSV curve at $s_x = 0.555i$, corresponding to $B_{qSV}(X; \delta) = 0$. Further, note the equal and opposite discontinuities in the qP and qSV curves at $s_x = 1.22i$, corresponding to X_\times where $B(X_\times; 0) = 0$ for both qP and qSV . This is necessarily at the same horizontal slowness where the elliptical qP and qSV curves (shown in gray) cross, the coordinates of the crossing point being given in (29).

APPLICATION TO f - k MIGRATION SCHEMES

For phase shift migration, one needs the vertical wavenumber k_z . For isotropic (or elliptically TI) media, the vertical

wavenumber is given by

$$k_z = \omega s_z = \frac{\omega}{\alpha_V} \sqrt{Z} = \frac{\omega}{\alpha_V} \sqrt{1 - X},$$

where α_V is the vertical wavespeed. The power of these rational approximations is that, for TI media, these expressions are replaced by

$$k_z = \frac{\omega}{\alpha_V} \sqrt{(1 - X)R_n(X)}. \quad (39)$$

In a homogeneous medium, only propagating modes, i.e., pre-critical waves, are required.

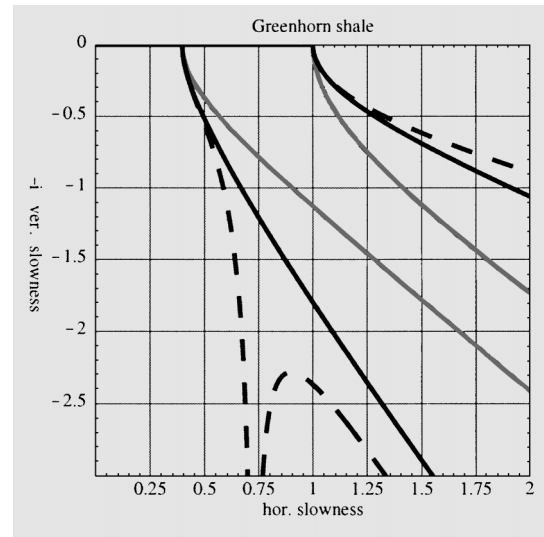


FIG. 6. Exact imaginary vertical slownesses and the first-order rational approximation for postcritical horizontal slowness (corresponding to $X > 1$ and $Z < 0$). Curves shown are for Greenhorn shale.

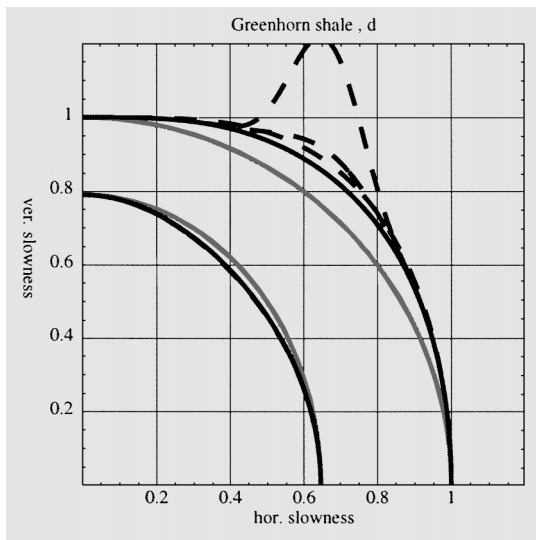


FIG. 5. The exact slowness curves and the first-, fifth-, and ninth-order rational approximations for a medium with $\gamma = 0.5$, $\epsilon_P = 0.2$, $\epsilon_A = -0.7143$. Because of the large value of γ , this large negative value of ϵ_A is negative enough for the qSV rational approximation to diverge over a significant range but is not negative enough for triplication to occur, as this value of ϵ_A is exactly the value for incipient triplication. In the diverging interval, the closest dashed curve to the exact solid curve is the first-order rational approximation, the next farthest is the fifth-order approximation, and the farthest is the ninth-order approximation. Since the anellipticity is negative, the even orders would lie inside the qSV curve.

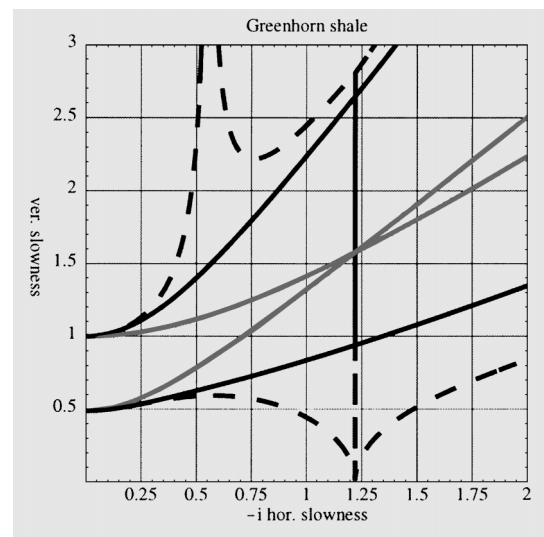


FIG. 7. Exact vertical slownesses and the first-order rational approximation along the imaginary horizontal slowness axis (corresponding to $X < 0$). Curves shown are for Greenhorn shale.

From zero-offset (poststack) data, Stolt single-mode migration requires ω in terms of k_x and k_z . The needed approximation can be obtained in a very similar manner as that carried out above, taking as a starting point the exact dispersion relation as given in equation (24) multiplied by $\Omega \equiv \omega^2$. Then, defining

$$K_X \equiv \omega^2 X, \quad K_Z \equiv \omega^2 Z,$$

equation (24) assumes the form

$$(K_X + K_Z - \Omega)^2 - [B(0)\Omega + [B(1; \delta) - B(0)]K_X] \\ \times (K_X + K_Z - \Omega) + \delta K_X(\Omega - K_X) = 0.$$

Introducing into this form an expansion about the elliptically anisotropic case, e.g.,

$$\Omega = K_X + K_Z + f_\Omega,$$

yields, after expansion in powers of f_Ω ,

$$[1 - B(0)]f_\Omega^2 - [[B(1; \delta) - \delta]K_X \\ + B(0)K_Z]f_\Omega + \delta K_X K_Z = 0. \quad (40)$$

As above, there is a sequence of rational approximations to the solution of this quadratic equation that vanishes when $\delta = 0$, based on the Taylor series expansion of $1 - \sqrt{1 - \zeta}$. The first-order rational approximation, after noting that $B(1; \delta) - \delta = B(1; 2\delta)$, is given by

$$f_\Omega \approx \frac{\delta K_X K_Z}{B(1; 2\delta)K_X + B(0)K_Z}. \quad (41)$$

Equivalently,

$$\Omega \approx \frac{[B(1; 2\delta)K_X + B(0)K_Z](K_X + K_Z) + \delta K_X K_Z}{B(1; 2\delta)K_X + B(0)K_Z} \\ = \frac{B(1; 2\delta)K_X^2 + [B(0) + B(1; \delta)]K_Z K_X + B(0)K_Z^2}{B(1; 2\delta)K_X + B(0)K_Z}. \quad (42)$$

Higher order approximations are easily derived as well.

DISCUSSION

We have derived a sequence of expressions giving an approximate relation for the vertical slowness squared as a sum of rational functions of the horizontal slowness squared and a dimensionless anellipticity parameter ϵ_A in a TI medium. We have compared our rational approximations with Dellinger et al.'s (1993) bielliptic approximation.

Our rational approximations are explicit, whereas Dellinger et al.'s bielliptic approximation to the dispersion relation is implicit. We have sacrificed numerical accuracy but gained algebraic clarity. Our purpose was to obtain a sequence of explicit approximations, sequentially regaining accuracy while losing clarity.

From equation (30), the first-order explicit formula for the approximate qP dispersion curve follows as

$$s_z^2 = \left[\frac{1}{c_{33}} - \frac{c_{11}}{c_{33}} s_x^2 \right] \frac{c_{33} - c_{55} + (c_{11} - c_{33})c_{55}s_x^2}{c_{33} - c_{55} + [(c_{11} - c_{33})c_{55} - E^2]s_x^2}, \quad (43)$$

where

$$E^2 = (c_{11} - c_{55})(c_{33} - c_{55}) - (c_{13} + c_{55})^2.$$

For $E^2 = 0$ the slowness curve is easily seen to be an ellipse. This elliptical approximation is a poor approximation for the usual transverse isotropy encountered in sedimentary basins for which the dimensionless anellipticity $\epsilon_A \ll 1$. Only the first power of the anellipticity appears in this expression. However, the approximation is much better than first order (in that anellipticity) since this approximation matches the curvature of the exact dispersion curve at the vertical and horizontal axes.

The accuracy of the low-order approximations differs from one another: the first-order rational approximation to the qP slowness curve is better than the bielliptic approximation, but the first-order qSV approximation is poorer. Dellinger et al.'s (1993) bielliptic approximation is still meaningful away from mild anisotropy; whereas for certain large enough negative values of anellipticity, the rational qSV approximation can diverge.

ACKNOWLEDGMENTS

We thank Oz Yilmaz for suggesting this problem and pointing out its potential application to seismic processing in anisotropic media. We also thank Leon Thomsen for his many valuable comments and the Center for Wave Phenomena for its partial support of this project.

REFERENCES

- Alkhalifah, T., and Tsvankin, I., 1995, Velocity analysis in transversely isotropic media: *Geophysics*, **60**, 1550–1566.
- Carrion, P., Costa, J., Pinheiro, J. E. F., and Schoenberg, M., 1992, Cross-borehole tomography in anisotropic media. *Geophysics*, **57**, 1194–1198.
- de Hoop, M. V., and de Hoop, A. T., 1994, Elastic wave up/down decomposition in inhomogeneous and anisotropic media: An operator approach and its approximations: *Wave Motion*, **20**, 57–82.
- Dellinger, J., Muir, F., and Karrenbach, M., 1993, Anelliptic approximations for TI media: *J. Seis. Expl.*, **2**, 23–40.
- Gassmann, F., 1964, Introduction to seismic travel time methods in anisotropic media: *Pageoph.*, **58**, 63–112.
- Helbig, K., and Schoenberg, M., 1986, Anomalous polarization of elastic waves in transversely isotropic media: *J. Acoust. Soc. Am.*, **81**, 1235–1245.
- Jones, E. A., and Wang, H. F., 1981, Ultrasonic velocities in Cretaceous shales from the Williston basin: *Geophysics*, **46**, 288–297.
- Miller, D. E., Leaney, S., and Borland, B., 1993, An in-situ estimation of anisotropic elastic moduli for a marine shale: 55th Mtg. and Tech. Exhib., EAEG, Expanded Abstracts, CO29.
- Payton, R. G., 1983, Elastic wave propagation in transversely isotropic media: *Martinus Nijhoff Publ.*
- Schoenberg, M., 1994, Transversely isotropic media equivalent to thin isotropic constituent layers. *Geophys. Prosp.*, **42**, 885–915.
- Schoenberg, M., and Sayers, C. M., 1995, Seismic anisotropy of fractured rock: *Geophysics*, **60**, 204–211.
- Thomsen, L., 1986, Weak elastic anisotropy: *Geophysics*, **51**, 1954–1966.
- , 1999, Converted wave reflection seismology over inhomogeneous, anisotropic media: *Geophysics*, **64**, 678–690.

APPENDIX A

CONVERGENCE OF SERIES (27) FOR NEGATIVE ANELLIPTICITY

The condition for convergence of the series in equation (27) is inequality (28). As discussed in the paragraph leading to equation (21), under the conditions of mild anisotropy, for qP $B > 0$ and for qSV $B < 0$ for $0 \leq X \leq 1$, while the numerator is positive except at the endpoints where it vanishes. Thus, the expression in equation (28) has a maximum value M at some value of X , say, at $X = X_{\max}$, between 0 and 1. Differentiating this expression yields, after setting the result to zero,

$$X_{\max} = \frac{B(0)}{B(0) + B(1; \delta)},$$

$$M = \frac{4X(1-X)|\delta|}{B^2(X; \delta)} \Big|_{X=X_{\max}} = \frac{|\delta|}{B(0)B(1; \delta)}. \quad (\text{A-1})$$

Thus,

$$M < 1$$

becomes the condition for convergence of the series in equation (27) for all precritical horizontal slownesses. It is necessarily satisfied for positive anellipticity; the condition must be analyzed in the context of mild anisotropy for negative anellipticity, $\delta < 0$, when, from equation (20),

$$B(1; \delta) = \begin{cases} \frac{(1 - \epsilon_P)(1 + \epsilon_P - \gamma)}{\gamma(1 + \epsilon_P)} + |\delta| & \text{for } qP, \\ -\frac{1 + \epsilon_P - \gamma}{1 - \epsilon_P} + |\delta| & \text{for } qSV. \end{cases} \quad (\text{A-2})$$

For qP -waves ($B(0) > 0, B(1; \delta) > 0$)

From equations (A-1) and (A-2),

$$M = \frac{|\delta|}{B(0) \left[\frac{(1 - \epsilon_P)(1 + \epsilon_P - \gamma)}{\gamma(1 + \epsilon_P)} + |\delta| \right]} < 1, \quad (\text{A-3})$$

which is satisfied by inspection for $B(0) \geq 1$ since

$$\frac{(1 - \epsilon_P)(1 + \epsilon_P - \gamma)}{\gamma(1 + \epsilon_P)} > 0$$

from mild anisotropy. Thus, we only have to consider the case $B(0) < 1$, i.e., $2c_{55} > c_{33}$. In the unlikely event that this is the case (since it means that the ratio of vertical shear velocity to vertical compressional velocity is greater than $\sqrt{2}/2$), $M < 1$ is equivalent to

$$|\delta| < \left[\frac{(1 - \epsilon_P)(1 + \epsilon_P - \gamma)}{\gamma(1 + \epsilon_P)} \right] \frac{B(0)}{1 - B(0)}. \quad (\text{A-4})$$

Equivalently, from the definition of $B(0)$ and δ in equation (20),

$$|\epsilon_A| < \frac{1 - \epsilon_P}{2\gamma - (1 - \epsilon_P)}$$

$$= \frac{\gamma}{1 + |\epsilon_P| - \gamma} + \frac{(1 - \epsilon_P)(1 + |\epsilon_P|) - 2\gamma^2}{[2\gamma - (1 - \epsilon_P)](1 + |\epsilon_P| - \gamma)}$$

$$= |\epsilon_{A_{\text{no trip}}}| + \frac{c_{33} \max[c_{11}, c_{33}] - 2c_{55}^2}{(2c_{55} - c_{33})(\max[c_{11}, c_{33}] - c_{55})}. \quad (\text{A-5})$$

Thus, the sign of the numerator of the second term on the right-hand side of inequality (A-5)—since the sign of the denominator is positive—determines whether the conditions of mild anisotropy automatically imply $M < 1$ for the case $2c_{55} > c_{33}$. If the numerator is nonnegative, ϵ_A satisfying the no-triplication condition of mild anisotropy implies that the inequality is satisfied and thus that $M < 1$. If the sign of the numerator is negative, i.e., $\sqrt{2}c_{55} > \sqrt{c_{33} \max[c_{11}, c_{33}]}$, then $M < 1$ is a more stringent condition than mild anisotropy; the more stringent condition is given by inequality (A-5). This case arises when, for $c_{11} < c_{33}$, the ratio of vertical shear velocity to vertical compressional velocity is greater than $\sqrt{\sqrt{2}/2} \approx 0.84$, while for $c_{11} > c_{33}$ the ratio of vertical shear velocity to the geometric mean of vertical and horizontal compressional velocities is greater than $\sqrt{\sqrt{2}/2}$.

For qSV -waves ($B(0) < 0, B(1; \delta) < 0$)

From equations (A-1) and (A-2),

$$M = \frac{|\delta|}{B(0) \left[-\frac{1 + \epsilon_P - \gamma}{1 - \epsilon_P} + |\delta| \right]} < 1, \quad (\text{A-6})$$

which is satisfied if and only if

$$|\delta| < \left[\frac{1 + \epsilon_P - \gamma}{1 - \epsilon_P} \right] \frac{-B(0)}{1 - B(0)}. \quad (\text{A-7})$$

Equivalently, from the definition of $B(0)$ and δ in equation (20),

$$|\epsilon_A| < \frac{\gamma}{2(1 - \epsilon_P) - \gamma}$$

$$= \frac{\gamma}{1 + |\epsilon_P| - \gamma} + \frac{\gamma[1 + |\epsilon_P| - 2(1 - \epsilon_P)]}{[2(1 - \epsilon_P) - \gamma](1 + |\epsilon_P| - \gamma)}$$

$$= |\epsilon_{A_{\text{no trip}}}| + \frac{c_{55}(\max[c_{11}, c_{33}] - 2c_{33})}{(2c_{33} - c_{55})(\max[c_{11}, c_{33}] - c_{55})}. \quad (\text{A-8})$$

As for the qP case, if the numerator of the second term on the right-hand side of inequality (A-8) is nonnegative (which is most unlikely since that nonnegativity requires $c_{11} \geq 2c_{33}$), the conditions of mild anisotropy automatically imply $M < 1$. If the sign of the numerator is negative (the expected situation), $M < 1$ is a more stringent condition than mild anisotropy; the more stringent condition is given by inequality (A-8). This inequality, in terms of dimensionless parameters, may be written as

$$\delta > -\frac{(c_{11} - c_{55})(c_{33} - c_{55})}{c_{33}(2c_{33} - c_{55})}$$

or

$$\epsilon_A > -\frac{c_{55}}{2c_{33} - c_{55}} = -\frac{\gamma}{2(1 - \epsilon_P) - \gamma}.$$

Often if ϵ_A is substantially negative, the series diverges for qSV and converges for qP . However, it is possible for it to converge for qSV and still diverge for qP or to diverge for both qP and qSV .

APPENDIX B

COMPARISON WITH DELLINGER, MUIR, AND KARRENBACH'S BIELLIPTIC APPROXIMATION FOR SLOWNESS CURVES

For either qP or qSV slowness surfaces, equation (19) with $f = 0$ allows us to express the case of elliptical anisotropy in dimensionless form as $X + Z = 1$ or, equivalently,

$$\frac{X^3 + 3X^2Z + 3XZ^2 + Z^3}{(X + Z)^2} = 1.$$

The bielliptic approximation to the slowness curve is a variation on this expression that ensures the slope of the squared slowness surface along the coordinate axes, i.e., at the anchor points $X = 0, Z = 1$, and $Z = 0, X = 1$ (equal to the curvature of the slowness surface at the anchor points), of the bielliptic approximate curve and of the exact curve are the same (Dellinger et al., 1993). To accomplish this, let

$$G(X, Z) \equiv \frac{X^3 + (2 - b_X)X^2Z + (2 - b_Z)XZ^2 + Z^3}{(X + Z)^2} - 1 = 0. \tag{B-1}$$

The fact that the total derivative of $G(X, Z)$ in equation (B-1) with respect to X and Z must vanish (since G is equal to a constant) enables us to find

$$\left. \frac{dZ}{dX} \right|_{X=0, Z=1} = b_Z, \quad \left. \frac{dX}{dZ} \right|_{Z=0, X=1} = b_X. \tag{B-2}$$

The exact values of $dZ/dX|_{X=0, Z=1}$ and $dX/dZ|_{X=1, Z=0}$ are given in equation (25). Thus, to preserve these slopes at normal and grazing incidence, the bielliptic approximation requires that

$$b_Z = -1 + \frac{\delta}{B(0)}, \quad b_X = -1 + \frac{\delta}{B(1; 0)}. \tag{B-3}$$

For the qP curve, b_X and b_Z are negative; for the qSV curve, b_X and b_Z can be negative or positive. Positive b_Z corresponds to a triplicating region around the vertical z -axis; positive b_X corresponds to a triplicating region around the horizontal x -axis.

These values of b_X and b_Z substituted into equation (B-1) yield Dellinger, Muir, and Karrenbach's (1993) bielliptic approximate slowness curves, i.e.,

$$G(X, Z) = \frac{X^3 + \left[3 - \frac{\delta}{B(1; 0)}\right]X^2Z + \left[3 - \frac{\delta}{B(0)}\right]XZ^2 + Z^3}{(X + Z)^2} - 1 = X + Z - 1 - \frac{\delta XZ}{(X + Z)^2} \left[\frac{X}{B(1; 0)} + \frac{Z}{B(0)} \right] = 0. \tag{B-4}$$

Because curvature at the anchor points is preserved, this approximation returns the correct horizontal and vertical zero-offset moveout velocity, as does our first-order rational approximation.

However, the problem with the bielliptic approximation is that it is implicit in X and Z and thus is as difficult to apply as the exact dispersion relation when Z as a function of X is required. The power of the bielliptic approximation comes from the fact that it is equally well suited for approximating the group velocity as a function of direction or the vertical component of the group velocity as a function of the horizontal component without the need to evaluate the associated slowness vector. To demonstrate, note that all group velocity vectors associated with real slowness vectors lie on a curve, the wave surface, which is polar reciprocal to the slowness curve. Further note that the polar reciprocal of an ellipse is also an ellipse. For elliptical anisotropy, the wave surface is given by $U + W = 1$ or, equivalently,

$$\frac{U^3 + 3U^2W + 3UW^2 + W^3}{(U + W)^2} = 1,$$

where

$$qP: \quad U \equiv \frac{v_{gx}^2}{c_{11}}, \quad W \equiv \frac{v_{gz}^2}{c_{33}};$$

$$qSV: \quad U \equiv \frac{v_{gx}^2}{c_{55}}, \quad W \equiv \frac{v_{gz}^2}{c_{55}}.$$

In similar fashion to the procedure for the slowness approximation, one approximates the wave surface by

$$V(U, W) \equiv \frac{U^3 + (2 - b_U)U^2W + (2 - b_W)UW^2 + W^3}{(U + W)^2} - 1 = 0 \tag{B-5}$$

and from the fact that the total derivative of V must vanish:

$$\left. \frac{dW}{dU} \right|_{U=0, W=1} = b_W, \quad \left. \frac{dU}{dW} \right|_{W=0, U=1} = b_U.$$

Thus, it remains only to evaluate $dW/dU|_{U=0, W=1}$ and $dU/dW|_{W=0, U=1}$ from the exact expression for group velocity (which is parameterized in terms of slowness). These derivatives are evaluated below. The results, from equations (B-16) and (B-19), are

$$b_W = -1 - \frac{\delta}{B(0) - \delta}, \quad b_U = -1 - \frac{\delta}{B(1; \delta)}. \tag{B-6}$$

Substituting these values into equation (B-5) gives the bielliptic approximation for the wave surface from Dellinger et al. (1993):

$$V(U, W) = \frac{U^3 + \left[3 + \frac{\delta}{B(1; \delta)}\right]U^2W + \left[3 + \frac{\delta}{B(0) - \delta}\right]UW^2 + W^3}{(U + W)^2} - 1 = 0.$$

In a more compact form,

$$U + W + \frac{\delta UW}{(U + W)^2} \left[\frac{U}{B(1; \delta)} + \frac{W}{B(0) - \delta} \right] = 1. \quad (\text{B-7})$$

This is a very good approximation for both qP - and qSV -wave surfaces except that it fails, by design, around triplications.

For both qP - and qSV -waves, to evaluate group velocity magnitude v_g as a function of group direction θ_g from equation (B-7), let $v_{gx} = v_g(\theta_g) \sin \theta_g$ and $v_{gz} = v_g(\theta_g) \cos \theta_g$ and solve the resulting linear equation on $v_g^2(\theta_g)$. Having $v_g(\theta_g)$ is particularly useful to evaluate traveltimes along a fixed (even if not precisely correct) raypath.

Evaluation of $dW/dU|_{U=0, W=1}$ and $dU/dW|_{W=0, U=1}$ from exact dispersion relation

The form of the dispersion relation suitable for either qP - and qSV -waves [equation (24)] is reproduced here:

$$F(X, Z; \delta) \equiv (X + Z - 1)^2 - B(X; \delta)(X + Z - 1) + \delta X(1 - X) = 0. \quad (\text{B-8})$$

Polar reciprocity of the wave and slowness surfaces is equivalent to the group velocity vector associated with a given slowness vector being given by $\mathbf{v}_g = \nabla_s / s \cdot \nabla_s$ so that the components of group velocity are

$$v_{gx} = \frac{\partial F}{\partial s_x} \left[s_x \frac{\partial F}{\partial s_x} + s_z \frac{\partial F}{\partial s_z} \right]^{-1}, \quad (\text{B-9})$$

$$v_{gz} = \frac{\partial F}{\partial s_z} \left[s_x \frac{\partial F}{\partial s_x} + s_z \frac{\partial F}{\partial s_z} \right]^{-1}.$$

Changing variables from s_x, s_z to X, Z yields

$$v_{gx} = \frac{\frac{\partial X}{\partial s_x} \frac{\partial F}{\partial X}}{s_x \frac{\partial X}{\partial s_x} \frac{\partial F}{\partial X} + s_z \frac{\partial Z}{\partial s_z} \frac{\partial F}{\partial Z}},$$

$$v_{gz} = \frac{\frac{\partial Z}{\partial s_z} \frac{\partial F}{\partial Z}}{s_x \frac{\partial X}{\partial s_x} \frac{\partial F}{\partial X} + s_z \frac{\partial Z}{\partial s_z} \frac{\partial F}{\partial Z}}.$$

After noting that for both qP and qSV ,

$$s_x \partial X / \partial s_x = 2X \quad \text{and} \quad s_z \partial Z / \partial s_z = 2Z,$$

the group velocity components become

$$v_{gx} = \frac{1}{s_x} \frac{X \frac{\partial F}{\partial X}}{X \frac{\partial F}{\partial X} + Z \frac{\partial F}{\partial Z}}, \quad v_{gz} = \frac{1}{s_z} \frac{Z \frac{\partial F}{\partial Z}}{X \frac{\partial F}{\partial X} + Z \frac{\partial F}{\partial Z}}.$$

Squaring and dividing by the appropriate elastic moduli (for qP or qSV) yields

$$U = \frac{X \left(\frac{\partial F}{\partial X} \right)^2}{\left[X \frac{\partial F}{\partial X} + Z \frac{\partial F}{\partial Z} \right]^2}, \quad W = \frac{Z \left(\frac{\partial F}{\partial Z} \right)^2}{\left[X \frac{\partial F}{\partial X} + Z \frac{\partial F}{\partial Z} \right]^2}. \quad (\text{B-10})$$

The needed expressions for $\partial F / \partial X$ and $\partial F / \partial Z$ are

$$\frac{\partial F}{\partial X} = (2 - B')(X + Z - 1) - B(X; \delta) + \delta(1 - 2X),$$

$$\frac{\partial F}{\partial Z} = 2(X + Z - 1) - B(X; \delta), \quad (\text{B-11})$$

where

$$B' = \frac{dB}{dX} = B(1; \delta) - B(0).$$

Then, using the vanishing of F for any possible wave, we find

$$X \frac{\partial F}{\partial X} + Z \frac{\partial F}{\partial Z} = (2 + B(0))(X + Z - 1) - B(X; 0). \quad (\text{B-12})$$

Substituting equations (B-11) and (B-12) into equation (B-10) yields

$$U = \frac{X[(2 - B')(X + Z - 1) - B(X; \delta) + \delta(1 - 2X)]^2}{[(2 + B(0))(X + Z - 1) - B(X; 0)]^2}, \quad (\text{B-13})$$

$$W = \frac{Z[2(X + Z - 1) - B(X; \delta)]^2}{[(2 + B(0))(X + Z - 1) - B(X; 0)]^2},$$

explicit expressions for U and W in terms of the corresponding X and Z (which satisfy the exact dispersion relation).

The derivative,

$$\frac{dW}{dU} \Big|_{U=0, W=1} = \lim_{\Delta X, \Delta Z \rightarrow 0} \frac{W(\Delta X, 1 + \Delta Z) - W(0, 1)}{U(\Delta X, 1 + \Delta Z) - U(0, 1)}$$

$$= \lim_{\Delta X \rightarrow 0} \frac{W(\Delta X, 1 + \Delta Z(\Delta X)) - 1}{U(\Delta X, 1 + \Delta Z(\Delta X))}, \quad (\text{B-14})$$

can be evaluated easily if $\Delta Z(\Delta X)$, i.e., ΔZ in terms of ΔX is known. From equation (25),

$$\Delta Z = \frac{dZ}{dX} \Big|_{X=0, Z=1} \Delta X + \mathcal{O}(\Delta X)^2$$

$$= \left[-1 + \frac{\delta}{B(0)} \right] \Delta X + \mathcal{O}(\Delta X)^2.$$

Thus,

$$X + Z - 1|_{X=\Delta X, Z=1+\Delta Z} = \Delta X + \Delta Z = \frac{\delta}{B(0)} \Delta X + \mathcal{O}(\Delta X)^2.$$

Substitution into equation (B-13) yields

$$U(\Delta X) = \frac{\Delta X[-B(0) + \delta]^2 + \mathcal{O}(\Delta X)^2}{B^2(0) + [2B(0)B' - 4\delta]\Delta X + \mathcal{O}(\Delta X)^2},$$

$$W(\Delta X) = \frac{B^2(0) + [2B(0)B' - 4\delta - B^2(0) + B(0)\delta]\Delta X + \mathcal{O}(\Delta X)^2}{B^2(0) + [2B(0)B' - 4\delta]\Delta X + \mathcal{O}(\Delta X)^2}. \quad (\text{B-15})$$

Further substitution into equation (B-14) then gives

$$\frac{dW}{dU} \Big|_{U=0, W=1} = -\frac{B(0)}{B(0) - \delta} = -1 - \frac{\delta}{B(0) - \delta}, \quad (\text{B-16})$$

the needed slope of the U, W curve at the vertical W -axis. Note that from equation (25)

$$\frac{dW}{dU} \Big|_{U=0, W=1} \times \frac{dZ}{dX} \Big|_{X=0, Z=1} = 1.$$

This constitutes a proof that the slopes at the vertical axis of the squared slowness and squared group velocity curves are reciprocal. A simple change of variables yields the result that

to know $\Delta X(\Delta Z)$, i.e., ΔX in terms of ΔZ . From equation (25),

$$\begin{aligned} \Delta X &= \frac{dX}{dZ} \Big|_{X=1, Z=0} \Delta Z + \mathcal{O}(\Delta Z)^2 \\ &= \left[-1 + \frac{\delta}{B(1; 0)} \right] \Delta Z + \mathcal{O}(\Delta Z)^2. \end{aligned}$$

Thus,

$$\begin{aligned} X + Z - 1 \Big|_{X=1+\Delta X, Z=\Delta Z} &= \Delta X + \Delta Z \\ &= \frac{\delta}{B(1; 0)} \Delta Z + \mathcal{O}(\Delta Z)^2. \end{aligned}$$

The procedure is exactly the same as that carried out above. Substitution into equation (B-13) yields

$$\begin{aligned} U(\Delta Z) &= \frac{B^2(1; 0) - [B(1; 0)B(1; \delta) + 2B(1; \delta)(B' + \delta) + 2(2 + B(0))\delta] \Delta Z + \mathcal{O}(\Delta Z)^2}{B^2(1; 0) - 2[B(1; \delta)(B' + \delta) + (2 + B(0))\delta] \Delta Z + \mathcal{O}(\Delta Z)^2}, \\ W(\Delta Z) &= \frac{\Delta Z B^2(1; \delta) + \mathcal{O}(\Delta Z)^2}{B^2(1; 0) - 2[B(1; \delta)(B' + \delta) + (2 + B(0))\delta] \Delta Z + \mathcal{O}(\Delta Z)^2}. \end{aligned} \quad (\text{B-18})$$

the curvatures at the vertical axis of the slowness and group velocity curves are also reciprocal.

The derivative,

$$\begin{aligned} \frac{dU}{dW} \Big|_{W=0, U=1} &= \lim_{\Delta X, \Delta Z \rightarrow 0} \frac{U(1 + \Delta X, \Delta Z) - U(1, 0)}{W(1 + \Delta X, \Delta Z) - W(1, 0)} \\ &= \lim_{\Delta Z \rightarrow 0} \frac{U(1 + \Delta X(\Delta Z), \Delta Z) - 1}{W(1 + \Delta X(\Delta Z), \Delta Z)}, \end{aligned} \quad (\text{B-17})$$

may be evaluated in the same way as the previous slope on the vertical axis was evaluated. This derivative is one over the slope of the U, V curve on the horizontal U axis. Here we need

Further substitution into equation (B-17) then gives

$$\frac{dU}{dW} \Big|_{U=1, W=0} = -\frac{B(1; 0)}{B(1; \delta)} = -1 - \frac{\delta}{B(1; \delta)}, \quad (\text{B-19})$$

the needed slope of the U, W curve at the horizontal U -axis. As was the case on the vertical axis, note from equation (25) that

$$\frac{dU}{dW} \Big|_{U=1, W=0} \times \frac{dX}{dZ} \Big|_{X=1, Z=0} = 1,$$

a proof that, at the horizontal axis as well, the slopes of the squared slowness and squared group velocity curves are reciprocal, as are the curvatures of the slowness and group velocity curves.